Sleep, 17(3):208–219

Measures of Location and Dispersion of Sleep State Distributions Within the Circular Frame of a 12:12 Light : Dark Schedule in the Rat

Ennio A. Vivaldi, Ursula Wyneken, *Manuel Roncagliolo, Adrián Ocampo and Ana M. Zapata

Departamento de Fisiología y Biofísica, Facultad de Medicina, Universidad de Chile, Santiago, Chile

Summary: Distributions within a 12:12 light : dark schedule of wakefulness (W), active sleep (AS), quiet sleep (QS) and of QS rich in delta (QSD) and in spindle (QSS) activities were evaluated for 52 days from 15 rats. Angular statistics were applied for each state by equating their hourly incidence to data distributed around a circle. Measures of location (mean angle, median angle, mode angle, maximum semicircle), dispersion (mean vector, standard deviation, quartile deviation), skewness and kurtosis were computed and their intra- and interindividual variabilities were compared. Mean angles (in hours and after lights-on) averaged 5.5 for QS, 8.6 for AS, 18.4 for W, 1.9 for QSD and 10.6 for QSS. Length of vectors, representing concentration around the mean angle, averaged 0.22 for QS, 0.36 for AS, 0.22 for W, 0.38 for QSD and 0.23 for QSS. Distributions of QS and W were closely related to the light–dark step function. QSD had a leptokurtic distribution, sharply rising at the beginning of the sleep-predominant phase, whereas AS and QSS had smoother distributions reaching maxima in its second half. In rodents as in humans, QSS and AS have opposite distributions to QSD. QSS may contribute to maintain sleep through the resting phase of the light–dark schedule after restorative function associated with delta activity has been fulfilled.
Key Words: Sleep—Quiet sleep—Active sleep—Circadian rhythms—Light entrainment—Delta waves—Sleep spindles—Angular statistics.

Sleep and wakefulness are adaptively linked to the light–dark cycle in most species in such a way that sleep restricts activity to either the day or the night. In a broader perspective, the timing of the daily occurrence of sleep, of its two internal states [active sleep (AS) and quiet sleep (QS)] and of the stages within quiet sleep provide a major context for physiological temporal organization.

The daily distributions of states and stages can also be regarded as an overt manifestation of the time course of the relative strength of brain mechanisms that control behavioral states. These mechanisms may in turn be subjected to diverse influences, such as those arriving from circadian oscillators, external zeitgebers or homeostatic regulatory processes.

Accepted for publication February 1994.
Address correspondence and reprint requests to Dr. Ennio A. Vivaldi, Departamento de Fisiología y Biofísica, Facultad de Medicina, Universidad de Chile, Avda. Independencia 1027, Casilla 70005, Santiago, Chile.

* Present address: Departamento de Fisiología, Facultad de Ciencias, Universidad de Valparaíso, Chile.

The present report is concerned with the distribution throughout a 12:12 light : dark schedule of behavioral states in the rat, as assessed by an automated data acquisition and scoring system (1) that identified the principal states of wakefulness (W), AS and QS and two subsets within QS.

The principal electrographic elements that occur in QS are delta waves and sleep spindles or sigma activity. Their relative presence is at the basis of the criteria for the classification of human QS into stages, which is assumed to have functional implications. The automated system used in the present study recognized two subsets within QS defined by a high density of delta (QSD) and sigma activity (QSS). In this way, the daily time course of these two patterns within QS could also be assessed.

Several facts are known concerning the distribution of states in the rat: wakefulness and sleep predominate in the dark and light phases, respectively; AS has a sinusoidal distribution that peaks late in the lights-on phase; and delta activity within QS concentrates at the beginning of the lights-on phase. We were interested

in examining what the appropriate quantitative indexes would be for assessing those and eventually other trends; what the typical values of those indexes would be; and how they should be expected to vary from one individual to another and from day to day within the same individual.

Accordingly, our main interest was to find simple and meaningful descriptors of location and dispersion of daily state distributions and to assess their intra- and interindividual variability. This was also considered a necessary background for interpreting results from experimental paradigms where the main dependent variable to be evaluated is the variation in 24-hour distribution of the sleep–wakefulness cycle (e.g. experiments designed to assess the response to alterations in the phase or in the photoperiod of the light–dark cycle). The description of state distributions in the rat is also of interest for comparative analysis with features of human sleep architecture that may have a general biological meaning, such as the tendency of QSD to concentrate at the beginning of the sleep-predominant phase (2).

We examined different procedures aimed at assessing the location and dispersion of states within the daily schedule. We first employed measures that provided a rather coarse overview of the distribution, such as the partition of the daily amount of each state between the light and dark phases and between the first and second halves of each phase. We then applied several techniques from the field of circular statistics, because hourly incidence of bins assigned to one state can be equated to grouping of angular data within a circle subdivided into 24 arcs of equal length. This allowed the typical hourly distributions of the three main states and of the two QS subsets to be estimated, their expected variability to be appraised and the summarizing value of different statistical descriptors to be compared.

METHODS

Recording environment

Fifteen male Sprague-Dawley rats, 250–300 g, under intraperitoneal chlornembutal 3 ml/kg anesthesia (3) were implanted with chronic electrodes at least 10 days before recordings began, following surgical procedures explained in detail in a previous report (4). Four cortical electrodes were placed 2 mm from the midline at 1 mm in front and 1, 3.5 and 6 mm behind the bregma, and one twisted three-wire depth electrode was aimed at the hippocampus. Each rat was housed in a 30-× 30-× 25-cm cage, placed within an 80-× 80-× 80-cm sound-isolated cube, under a light–dark schedule with lights on from 0800 to 2000 hours local time. (Throughout this report, the time of the day is expressed as time elapsed since the moment lights were turned on, not as local time.) Light intensity was approximately 700 lux. Two cortical, one hippocampal and one muscle derivations were brought through a slip-ring assembly to corresponding channels of a polygraph where filters and gains were set according to the specific signals to be detected. From the auxiliary outputs of the amplifiers the signals were sampled by a microcomputer through an 8-bit analog-to-digital converter. The microcomputer was also equipped with a board that provided a real-time clock and input/output lines. One output line controlled illumination of the cages, ensuring synchronization between light schedule and data tables.

Data acquisition software

The goals of the data acquisition program were, firstly, to detect cortical delta and sigma activities, hippocampal theta rhythm and muscle spikes; secondly, to quantify the incidence of those elements in 15-second bins; and, thirdly, to build and store a table whose columns were the four relevant elements and whose rows were the time bins.

A detailed account of the program can be found elsewhere (1). In summary, the software sampled the four channels at a 500-Hz rate, it determined the period and amplitude of each full waveform from one upward zero-crossing to the next, and it decided whether the detected waveform was within the period and amplitude windows corresponding to the element it was looking for in that channel. In one cortical channel the relevant element was the occurrence of single delta waves (1–4 Hz) and in the other it was a train of three consecutive sigma waves (11–16 Hz). In the hippocampal channel the program looked for trains of eight theta waves (4–8 Hz), and in the muscle channel it looked for muscle spikes or movement artifacts.

The software quantified the amount of detected elements occurring in each successive 15-second bin and built a table with that data. Because each cell contained the incidence of a given element in a given bin, data tables corresponding to 1 day were made of 4 columns, one for each relevant element, and 5,760 rows, one for each 15-second bin. Data acquisition and processing were interrupted only momentarily to store data tables as disk files. Stored files could be imported later to conventional spreadsheet, statistical or graphics software.

State diagnosis

Each bin was assigned to one of three mutually exclusive states: QS, AS and W. Automated state scoring

was performed by means of a simple logic formula that related the actual values of the four variables in a given bin with the respective thresholds for that variable, as explained in a previous report (5). The thresholds had been defined previously for each rat after comparing the visual scoring of a sample chart tracing with its corresponding computer-generated data table. If muscle was above its threshold, the bin was ascribed to W irrespective of the other three variables. If theta was above its threshold, the bin was assigned to AS irrespective of delta and sigma. If either delta or sigma or both were above their thresholds, it was scored as QS. If no variable was above threshold, the bin was assigned to W. A four-column daily data table was thus transformed into a unidimensional array, a sequence of 5,760 bins, with each bin assigned to one of three possible behavioral states.

Two subsets were obtained from the bins that had been scored as QS and consisted of those bins with a higher incidence of delta activity (QSD) and those with a higher incidence of sigma activity (QSS). A frequency distribution of QS bins was generated in terms of incidence of delta activity, that is, how many QS bins had 0, 1, 2, . . . , etc., delta waves. A second delta threshold was then determined that would leave approximately 20% of QS bins above it. An analogous procedure was followed to determine the second threshold for sigma. It should then be noted that the thresholds used to score W, QS and AS were chosen through a procedure that attempted to replicate the logic of human scoring of a polygraphic recording, so they referred to an external standard. On the other hand, the thresholds for QSD and QSS were chosen to select that fifth of the population of QS bins that had either a particularly high density of delta or sigma activity, so they were relative to an internal distribution. It should also be noted that QSD and QSS, unlike W, QS and AS, were not defined to be mutually exclusive.

Daily data base

We report data corresponding to 52 days from 15 rats. For data analysis on a daily scale we added the incidence of each state across the 240 bins that constituted each hour, so that the original data arrays that had a 15-second resolution were grouped into tables that had a resolution of 1 hour, starting with the 1st hour of lights on. Therefore, the data for 1 day were condensed into a matrix of 24 rows × 5 columns, one row for each hourly aggregation and one column for each of the three principal states and the two QS subsets. Each cell thus contained the number of bins assigned to a given state in a given hour. (It follows that in each row the sum of the W, QS and AS cells had to be 240 and that the QSD or QSS cells could not exceed the value in the QS cell.) A second version of these tables was normalized as columnwise percentages, with each cell representing the fraction of the daily total of the state that occurred in that hour. Depending on the type of analysis, the raw or normalized tables were used. Figure 1 is a graphic display of such tables for 3 days from one rat and for the hourly averages of those 3 days. Throughout this report the time of day or angular direction is expressed in hours and fraction of an hour, using 0.0 as the time when lights are turned on.

Statistical analysis

Daily tables constituted the working units for statistical analysis. Spreadsheet formulas were developed that operated on the daily tables in order to calculate several variables for each state in each day. Those variables represented diverse ways of assessing the distribution, location and dispersion of the five states within the 12:12 light : dark schedule. For each state the following variables were calculated: total amount in the 24 hours, fraction occurring during each quadrant, mean angle, angular median, angular mode, center of the semicircle of maximum incidence, mean vector, angular standard deviation, quartile deviation, percentage of daily total occurring in the mode hour and percentage of daily total occurring in the semicircle of maximum incidence.

For each variable an average and a standard deviation were calculated for every state in each rat. The mean of individual averages was obtained as a global indicator of the population mean. The standard deviation of individual averages provided an index of interindividual variability. The mean of individual standard deviations provided an index of intraindividual variability.

For a preliminary appraisal of the daily distribution of states, the subtotals per quadrant, that is, the first and second halves of the light and of the dark phases, were obtained. The partitions between the light and dark phases and between the first and second half of each phase provided a coarse idea of the eventual tendencies of the distributions. The fraction occupied by AS, QSD and QSS within the total amount of sleep occurring in each quadrant was also computed.

A subsequent analysis applied techniques from the field of circular statistics. Those techniques are explained in detail in Mardia (6) and Batschelet (7) and are summarized in Zar (8).

The statistics were obtained independently for each of the five states. In each case, n is the total number of bins in the day that were scored as belonging to a given state. The incidence of bins that occurred during the hour i, and $i = 0, 1, .. 23$ ($i = 0$ being the 1st hour after lights are turned on), is expressed as f_i. The mode

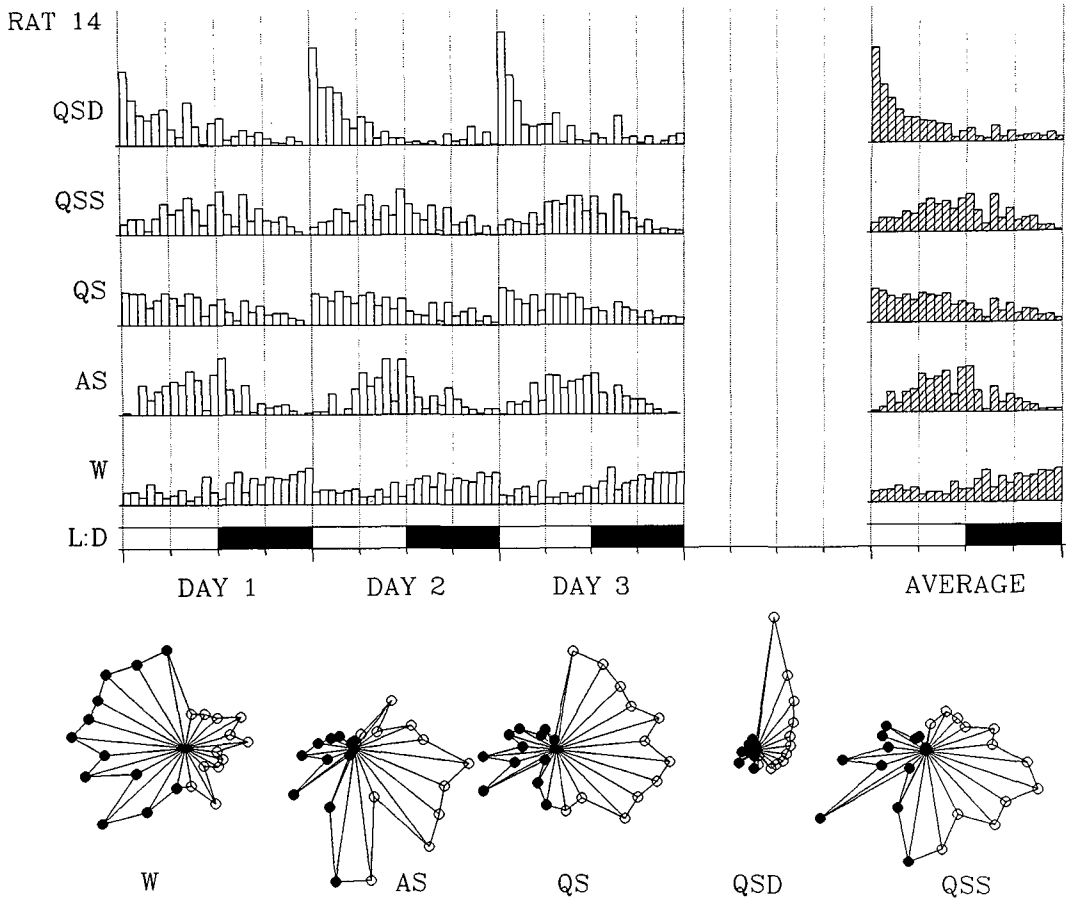

FIG. 1. Hourly distributions of wakefulness (W), quiet sleep (QS), active sleep (AS), QS rich in delta activity (QSD) and QS rich in sigma activity (QSS), throughout 3 consecutive days, representing a graphic display of a sample of the data tables submitted to statistical analysis. Data for each state have been normalized as percentage of daily total. (As a reference, the full height of each state graph corresponds to 20%.) Hourly averages for each state are shown at the right as hatched bars and below as circular graphs. In circular graphs hourly incidences are represented as radii with lengths relative to a unit value that is equal to the mode. Clockwise, the open circles at the right half of each graph represent the hours of the light phase and the filled circles at the left half, those of the dark phase.

hour of a state is that hour with the highest incidence of the state. (As a reference, if a state were evenly distributed throughout the 24 hours, each hour would contain 4.16% of the daily total.)

For grouped statistical calculations, each hourly group of bins f_i is assumed to be located at the angle A_i, which is the midpoint of the hour i expressed in radians:

$$A_i = (i + 0.5)*\pi/12$$

The mean vector is the most prominent statistic used to describe a circular distribution. It can be better visualized by comparing how the physical concept of the center of gravity is applied to linear and to circular distributions. If linear data are conceived as unit weights distributed along a weightless horizontal bar, then the mean is at the center of gravity of that bar. If circular data are conceived as unit weights distributed around a weightless horizontal disc, then the center of gravity is at a point within the disk located at a certain distance and angle from its center, corresponding to the length and angle of the mean vector.

To compute the length and angle of the mean vector, its rectangular coordinates C and S are calculated as the mean cosine and the mean sine of the data points. In the case of grouped data the formulas become:

$$S = 1/n \sum f_i \sin A_i$$

$$C = 1/n \sum f_i \cos A_i$$

The length of the mean vector, r, and the mean angle expressed as hour of the day, x, are then defined as:

$$r = (S^2 + C^2)^{1/2}$$

$$x = \arctan(S/C)*12/\pi \quad [+12, \text{ if } C < 0]$$

The numeric values of the mean vector length and angle are similar to those of the estimated amplitude and acrophase parameters of a rhythm of known period

obtained by least-squares fitting of a cosine function to a series of observations (9).

The mean vector can be considered as a measure of concentration around a mean direction, because it becomes larger as data points are more clustered around the mean angle. Accordingly, the definition of the angular standard deviation, s, as a measure of dispersion is derived from the complement to one of r:

$$s = [2 \cdot (1 - r)]^{1/2} \cdot 12/\pi$$

The location and dispersion of circular distributions, expressed by the mean angle and the angular standard deviation, are related to the first trigonometric moment. Measures of skewness (symmetry) and kurtosis (flatter or sharper peak) of circular distributions can be derived from the sine and cosine, respectively, of the second trigonometric moment. The probability density function known as the von Mises distribution plays for circular data a similar role to that of the normal distribution for linear statistical analysis. The shape of a particular von Mises distribution is given by its concentration parameter. The concentration parameter is also related to the length of the mean vector.

The hypothesis that a sample comes from a population randomly distributed around the circle, as opposed to a population exhibiting one-sidedness or directedness, can be examined by the Rayleigh test. This test compares the value z of the sample with the critical value $z_{\alpha,n}$. The value z is calculated from r and n:

$$z = n \cdot r^2$$

The circular median or median angle is a statistic analogous to the median of linear data. It is related to the particular diameter of the circle that divides the data into two groups of equal size. The median angle is the angle indicated by the radius on that diameter pointing towards the side with the majority of data points. Because n is the total number of bins in the 24 hours assigned to a given state, we operationally determined the median angle by first locating that hour which added to the previous 11 hours yielded a sum greater than or equal to $n/2$, whereas the sum of the previous 12 hours was less than $n/2$, and we then found the fraction of that hour that made the partition equal to $n/2$. In this computation the hour 0 is assumed to follow the hour 23. Each of the two half circles created by the median angle can in turn be divided into moieties containing $n/4$ bins, a process that determines the angles corresponding to quartiles Q_1 and Q_3. The quartile deviation is then defined as the arc length from Q_1 to Q_3 that contains the median angle. A smaller arc length indicates that data points are more clustered around the median angle.

The semicircle of maximum incidence refers to that grouping of 12 consecutive hours that yields the highest sum. It is a measure that has also been employed to determine if a sample comes from a population randomly distributed around a circle, as in the Hodges-Ajne test of directedness (6,7). Borbély has applied a similar test to circadian data as the A statistics (10). The sum of the 12 hours of the maximum semicircle can be expressed as percentage of the daily total and the location of the semicircle can be indicated by the hour at its center.

RESULTS

A graphic display of an example of the data tables containing the hourly distributions of bins assigned to each state for 3 days from one rat is presented in Fig. 1. The figure also shows the hourly averages of the 3 days, both as bar graphs and as angular graphs.

Figure 2 shows the hourly averages of each state in each rat and the hourly grand averages. By simple inspection of the hourly grand averages, some of the main features of state distributions become apparent. W and QS have a two-step distribution closely coinciding with the light–dark cycle. QSD has a sharp increase at the beginning of the lights-on sleep-predominant period followed by a slower decline. AS and QSS follow distributions that are more sinusoidal, with QSS being the smoothest and both having maxima in the second half of the lights-on period.

Several variables related to the distribution, location and concentration of states were calculated from the daily data tables. Table 1 summarizes results of 15 variables for the three main states and the two QS subsets. The mean of individual averages, the standard deviation of individual averages and the mean of individual standard deviations for each variable are indicated.

Amount of W, QS and AS per day

As shown in Table 1, row A, percentages of the day occupied by W, QS, and AS closely approximate a ratio of 5:4:1. The interindividual ranges of the percentage of the day occupied by a state were 36–44 for QS, 8–12 for AS and 47–55 for W. Intraindividual variabilities were significantly smaller; the analysis of variance by rats yielded an F of 8.1 for QS, 14.1 for AS and 8.0 for W.

Distribution through the light-dark schedule

As indicated in Table 1, row F, approximately ⅔ of W occurs in the dark phase and ⅔ of QS, AS and QSD occurs in the lights-on phase. QSS preference for the lights-on phase is also evident but less marked.

In Table 1, rows B–E, the quadrants 00–05 and 06–

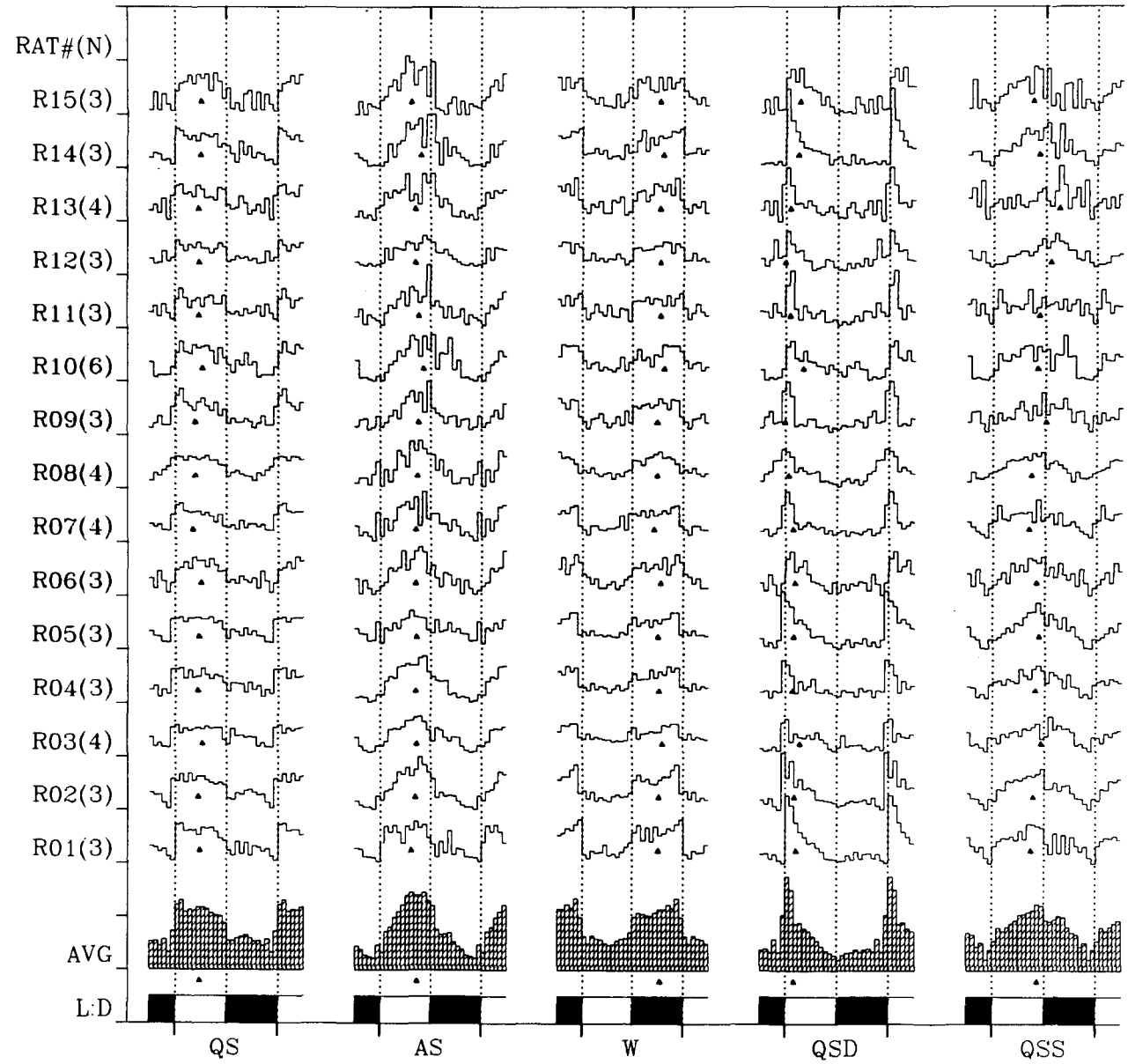

FIG. 2. Line graphs represent the hourly averages of N days for a given rat and for a given state, whereas hatched bars at the bottom represent hourly averages across rats. The first 6 hours of light and the last 6 hours of darkness are double-plotted to help the visual appraisal of dark to light transition. Tick marks denote zero levels. Data are normalized so that the distance between two tick marks equals 10% of the daily total in line graphs and 5% of the daily total in bar graphs, except for QSD where those values are 14% and 7%, respectively. Small triangles indicate the time of day corresponding to the mean angles of circular distributions.

11 represent the first and second halves of the lights-on phase, whereas 12–17 and 18–23 represent the first and second halves of the dark phase. Taken together in that order, the grand averages of the percentages of a state's daily total occurring in each quadrant are 35:31:18:16 for QS, 25:41:23:10 for AS, 17:17:31:35 for W, 46:18:14:22 for QSD and 23:34:28:15 for QSS. A graphic representation of these distributions by quadrants for each rat is shown in Fig. 3.

When averages by quadrants in each rat were ranked, two kinds of patterns appeared. QS and W had two quadrants of high incidence, corresponding to the light and the dark phases, respectively, and two quadrants of evenly lower incidence. For both states, the differences between their two high-incidence quadrants were moderate but consistent, because QS is higher in the first half of the lights-on phase and W is higher in the second half of the dark phase.

A different pattern was seen for QSD and AS. They clearly predominated in one quadrant, the first and second halves of the lights-on phase, respectively. Their incidence then diminished fairly evenly in the two

TABLE 1. *Amount of each state and measures of distribution, location and concentration*

	QS	AS	W	QSD	QSS
Amount of each state					
A. Percent occupied by state	39.2 ± 2.4 (1.1)	9.8 ± 1.3 (0.5)	51.0 ± 2.8 (1.3)	10.6 ± 1.1 (0.8)	8.8 ± 1.2 (0.8)
Light : dark distribution					
B. Hours 00–05 (light)	35.2 ± 1.9 (1.4)	25.7 ± 4.2 (2.6)	17.0 ± 2.1 (1.3)	46.6 ± 9.0 (4.6)	23.4 ± 3.1 (2.2)
C. Hours 06–11 (light)	31.5 ± 2.0 (1.6)	41.9 ± 3.4 (3.5)	16.8 ± 1.8 (1.6)	18.3 ± 3.1 (2.6)	33.9 ± 4.8 (2.2)
D. Hours 12–17 (dark)	17.7 ± 1.9 (1.1)	22.4 ± 3.6 (2.9)	31.2 ± 2.2 (1.3)	13.1 ± 3.8 (2.6)	28.1 ± 3.9 (2.6)
E. Hours 18–23 (dark)	15.6 ± 2.8 (1.5)	10.0 ± 3.4 (2.6)	35.1 ± 2.3 (1.6)	21.9 ± 8.7 (2.6)	14.6 ± 4.0 (1.9)
F. Percent in light phase	66.7 ± 3.3 (1.8)	67.6 ± 4.9 (3.4)	33.8 ± 3.3 (1.8)	64.9 ± 9.4 (4.1)	57.3 ± 6.0 (2.5)
Measures of location					
G. Mean angle	5.5 ± 0.7 (0.4)	8.6 ± 0.7 (0.4)	18.4 ± 0.6 (0.4)	1.9 ± 1.2 (0.5)	10.6 ± 1.8 (0.8)
H. Median angle	5.6 ± 0.8 (0.5)	8.7 ± 0.7 (0.5)	18.6 ± 0.6 (0.3)	1.6 ± 1.0 (0.6)	10.5 ± 1.8 (0.7)
I. Mode angle	3.6 ± 2.2 (2.0)	9.6 ± 1.5 (1.9)	19.2 ± 1.4 (2.9)	0.5 ± 1.0 (0.7)	11.8 ± 2.3 (2.2)
J. Center maximum semicircle	5.5 ± 0.6 (0.2)	8.2 ± 1.0 (1.1)	17.8 ± 0.5 (0.3)	3.0 ± 2.0 (1.1)	10.5 ± 2.1 (1.3)
Measures of concentration					
K. Mean vector	0.22 ± 0.04 (0.02)	0.36 ± 0.07 (0.04)	0.22 ± 0.04 (0.02)	0.38 ± 0.09 (0.07)	0.23 ± 0.06 (0.03)
L. Angular standard deviation	4.75 ± 0.13 (0.06)	4.31 ± 0.24 (0.15)	4.75 ± 0.12 (0.06)	4.22 ± 0.33 (0.23)	4.74 ± 0.19 (0.09)
M. Quartile deviation	8.9 ± 0.7 (0.6)	7.2 ± 1.0 (0.8)	8.9 ± 0.5 (0.7)	6.3 ± 1.3 (1.2)	9.2 ± 0.9 (1.0)
N. Percent in mode hour	7.5 ± 0.6 (0.4)	11.1 ± 1.1 (1.1)	7.7 ± 0.5 (0.4)	14.9 ± 2.5 (2.0)	9.5 ± 1.1 (0.7)
O. Percent in maximum semicircle	67.7 ± 2.8 (1.6)	74.5 ± 4.7 (3.1)	67.1 ± 3.0 (1.5)	75.5 ± 5.4 (3.7)	66.1 ± 3.7 (2.0)

For each variable three values are shown for each state: mean of individual averages ± standard deviation of individual averages (mean of individual standard deviations). Variable A represents the fraction of the day occupied by a state expressed as percentage. Variables B–F and N–O represent a fraction of the daily total of a state expressed as percentage. Variables G–J represent an angular direction expressed as hour of the day where 0.0 is the time lights are turned on. Variable K is an adimensional value between 0 and 1. Variables L and M represent a time interval expressed in hours.

quadrants adjacent to the preferred one and became lowest in the opposite quadrant. These patterns were reflected by the means of ratios between the quadrants with the highest and lowest incidence in each rat: 2.4 for QS, 4.6 for AS, 2.2 for W, 4.2 for QSD and 2.6 for QSS.

Relative incidence of sleep states per quadrant

The incidence of AS, QSD and QSS in each quadrant was expressed as a fraction of total sleep in that quadrant in order to better perceive the time course of the relative propensity toward these states within sleep. Results are shown in Fig. 4. AS occupies almost 25% of the sleep occurring in the second half of the lights-on phase and in the first half of the dark phase, but only 15% in the other two quadrants. On the other hand, QSD occupies some 30% or more of the sleep occurring at the end of the dark phase and at the beginning of the lights-on phase, but 15% or less in the other two quadrants. The specific incidence of QSS is particularly high in the first half of the dark phase.

Semicircle of maximum incidence

To assess the tendency of a given state to concentrate on one side of the 24-hour circle, not necessarily coinciding with the dark or light phase, we looked for the 12 consecutive hours where the state reached its maximum incidence. As indicated in Table 1, row O, that fraction was close to ⅔ for QS, W and QSS and to ¾ for AS and QSD. The location of the maximum semicircle for QS and W either coincided or anticipated in 1 hour their preferred phase. As compared to QS, the semicircle was shifted to an earlier phase in the case of QSD and to a later phase in the cases of AS and QSS. The variability of the location and the percentage contained within the semicircle was higher for AS, QSD and QSS than for QS and W.

Angular measures of location

The average mean angle of QS anticipates in about ½ hour the midpoint of the lights-on period and that of W is delayed ½ hour with respect to the midpoint of the dark period, as can be seen in Table 1, row G, and in Fig. 5. The mean angle of QSD occurs early in the lights-on period, that of AS occurs midway through its second half, and that of QSS is located later in the second half. Both intra- and interindividual variabilities of the mean angle are small for QS, AS and W and large for QSS. QSD has a moderate intraindividual and a larger interindividual variability.

The median angles for all states were remarkably close to the mean angles, but, even if differences were small, they were also consistent, particularly in the

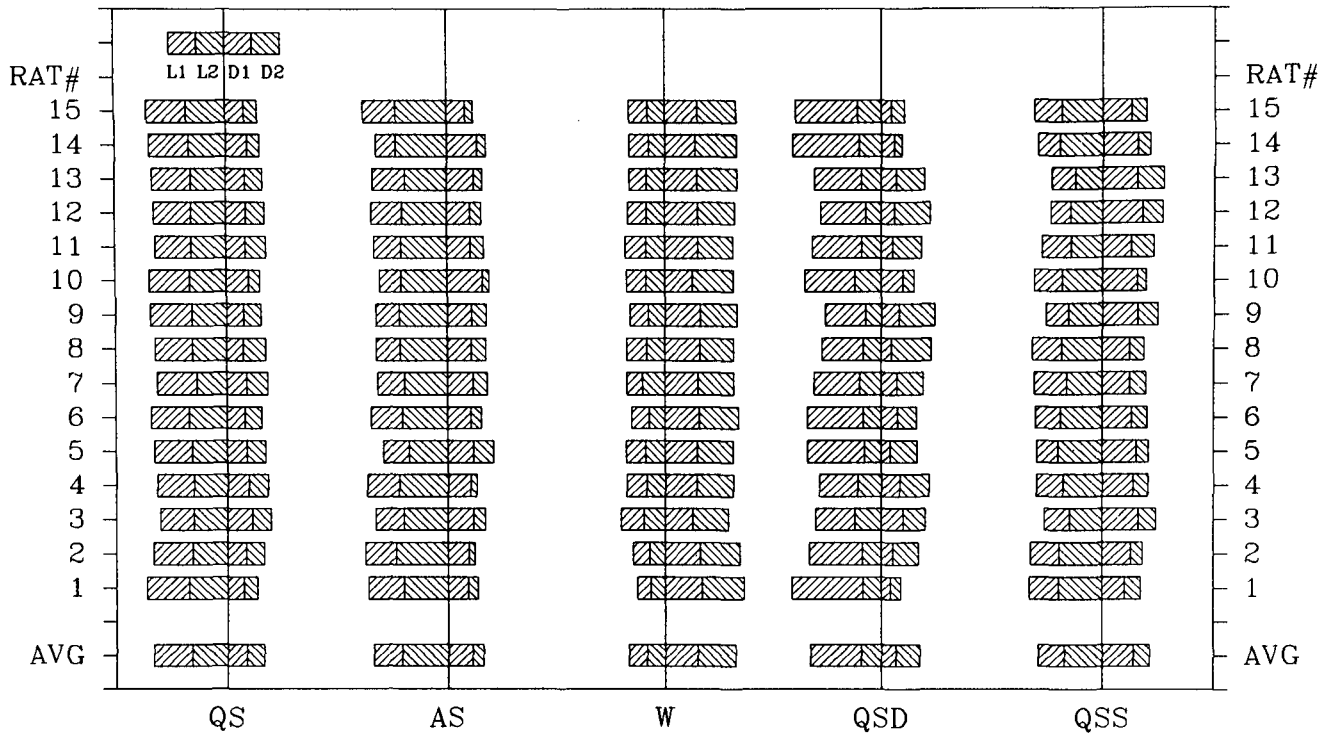

FIG. 3. Daily distributions by quadrant. Each rectangle represents the average distribution for a given rat and for a given state, with the bottom line representing the averages across rats. Rectangles are of equal length and each of its four parts are proportional to the fraction of the state daily total that occurs in the corresponding quadrant, as indicated in the inset at top left. Rectangles are vertically aligned at the border corresponding to light-off time in order to facilitate the appraisal of light/dark partitions.

cases of W where the mean angle occurs before the median angle and of QSD where it occurs after. On the other hand, the mode angles could differ considerably from the mean angle and showed a much higher intra- and interindividual variability. In the cases of QS and QSD, the mode angle is located earlier than the mean angle; in the cases of the other states, it is located at a later time.

The relative positions of these three measures of central tendency is such that in QSD the mode angle is followed by the median angle and then the mean angle, whereas in AS and W that order is reversed.

Angular measures of concentration

The lengths of the mean vectors, shown in Table 1, row K, are indicators of the tendency of data points to concentrate close to the mean angle. AS and QSD have greater mean vectors than the other states. The Rayleigh test, which considers the value of the mean vector and the total number of observations to test the null hypothesis of random circular distribution, rejected that hypothesis at the 0.01 level for the five states in all rats.

The tendency to cluster around the mean angle can be represented by the length of the mean vector or by two other related parameters, the angular standard deviation, shown in Table 1, row L, and the concentration parameter. Table 1, row K, indicates that the mean vector value of QSD is 0.38 and that of AS is 0.36. Those values would correspond to concentration parameters of 0.82 and 0.77, respectively. According to the tables of the von Mises distribution function (6,7), for a concentration parameter of 0.80, half of the observations would occur within some 6.6 hours around the mode angle. A mean vector of 0.22—like the one QS, W and QSS have—is equivalent to a concentration parameter of 0.45 that would gather half the observations in some 8.8 hours.

The arc length around the median angle that actually contains half of the total incidences of a given state is the quartile deviation. Table 1, row M, shows that the actual values are 6.3 hours for QSD and 7.2 for AS, whereas the other three states have results close to 9 hours. The quartile deviation of QSD reached values at low as 3.1 hours in a given day and as low as 3.8 for the hourly average of a given rat. Comparison of the kurtosis indexes confirmed that QSD was the state with the strongest tendency to concentrate in a short time span.

Table 1, row N, shows the percentage of a state daily total that occurs during the mode hour, that is, the maximum value reached by the hourly distribution curve. It is highest for QSD, with an average close to

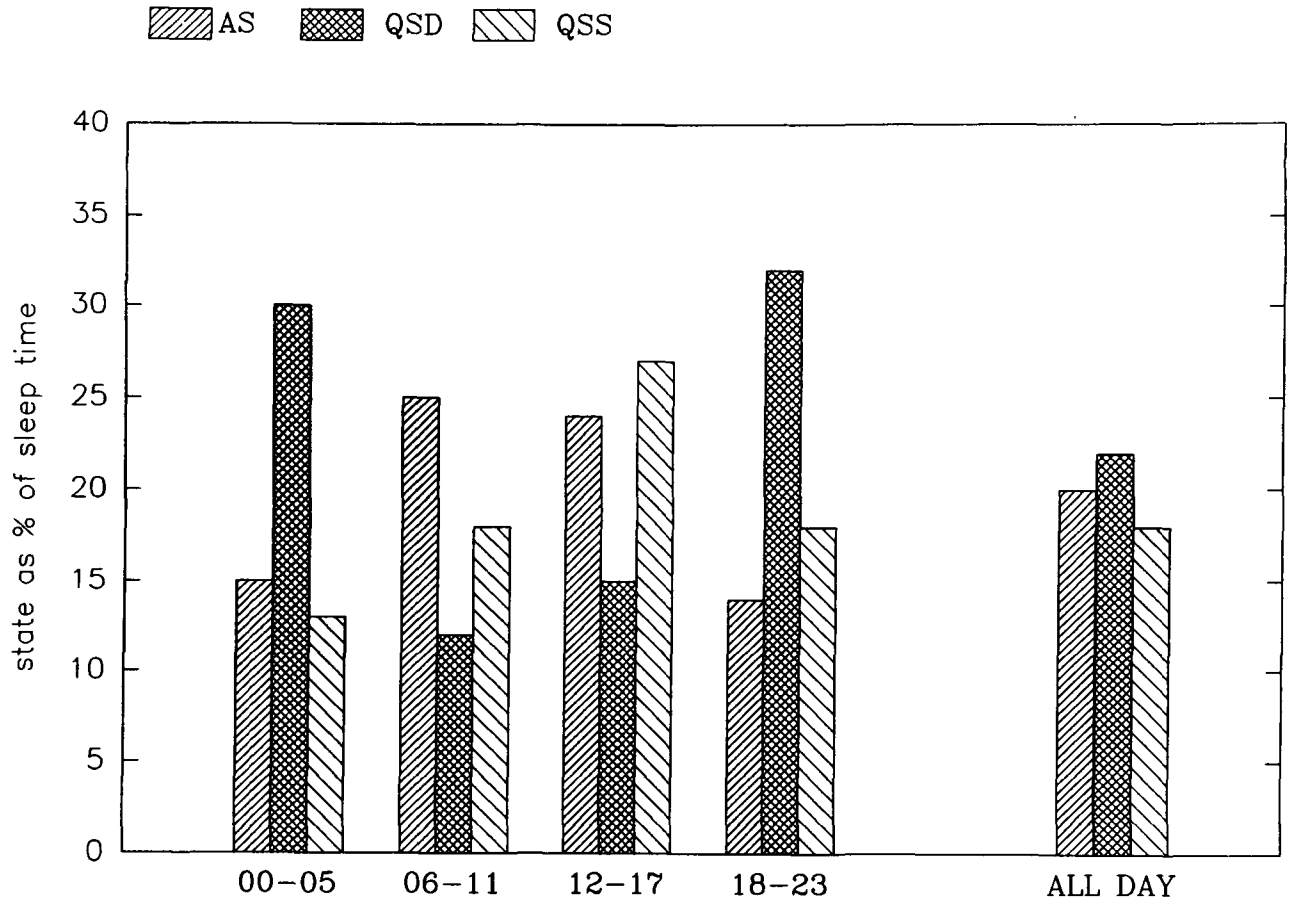

FIG. 4. Bars represent the percentage that AS, QSD and QSS occupy of sleep time within each quadrant and through the 24 hours. The graph emphasizes that within sleep QSD is predominant in the second half of the dark phase and first half of the light phase and that the reverse is true for AS. QSS is predominant within sleep occurring at the fist half of the dark phase.

15 (the maximum observed value for an individual day was 25), followed by AS and QSS. The average minimum value, not shown in the table, was 1.2 for W, 0.5 for QS and near zero for the other three states. W was not absent for a full hour in any single day.

Hourly grand averages of states

The hourly grand averages of the distributions of the five states are represented in bar graphs at the bottom of Fig. 2. Note that QSD is at a reduced scale compared to the other states, its maximum value being 12.5 percent of the daily total occurring in 1 hour. The locations of the mode angle of QS at the beginning of the lights-on period and that of W at the end of the dark period become more evident, reflecting a moderate skewness of those distributions. The average curve of AS is more concentrated around its mean angle than are individual ones; it has a sharper rise than fall, with a step decline at the beginning of the dark period and a marked nadir at the end of the dark period. The average QSD curve has a leptokurtic and skewed shape, with a very sharp rise and a shouldered decline. The QSS curve is fairly symmetric and has a smooth maximum that is reached towards the end of the lights-on phase.

DISCUSSION

In this report we described the distribution of sleep states through a 12:12 light:dark schedule and computed several measures of location and concentration, employing circular statistics as if hourly incidence corresponded to angular data within a circle subdivided into 24 arcs. The goal was to reach simple and meaningful measurements of the location, dispersion, skewness and kurtosis of sleep-state distributions.

The main states within sleep, QS and AS, have been described in many species, along with implications concerning their specific mechanisms and functions. The guidelines for classifying QS into substates or stages in humans (11,12) emphasize the relative amount of delta waves, with its implication for depth of sleep and for the typical progression of patterns seen as human sleep unfolds at the beginning of the night. These guide-

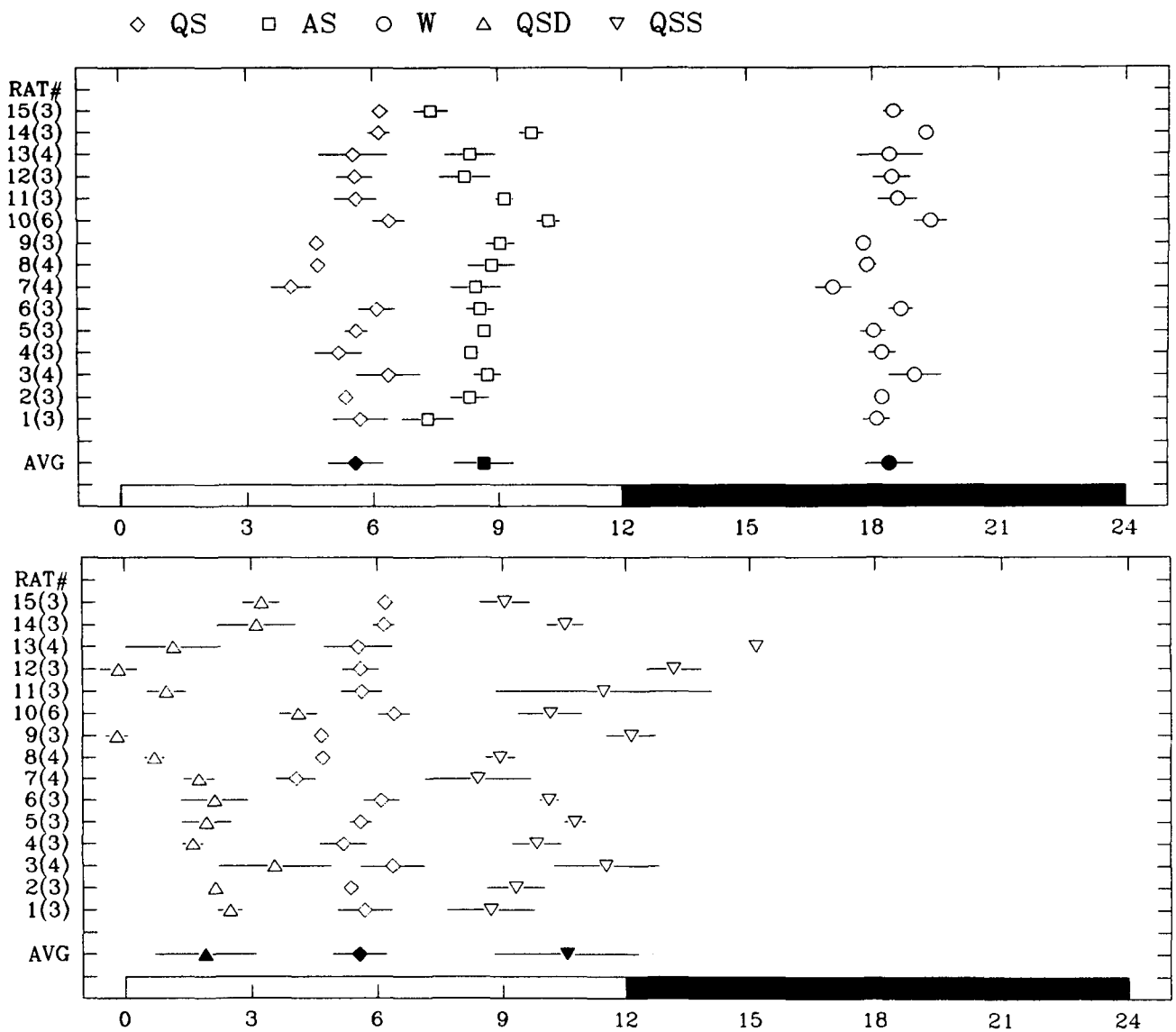

FIG. 5. Location of mean angles. QS, AS and W are shown above and QS, QSD and QSS are shown below. Symbols corresponding to each state are indicated. Filled symbols represent averages across rats. Horizontal lines represent standard deviations of mean angles. QS values are plotted in both graphs for comparison with the other two principal states and with its own two subsets.

lines have been also applied to rats (13–18), mice (19,20), guinea pigs (21), cats (22–24) and other species (14,25). In our report, after establishing fixed criteria for W, QS and AS, we extracted two subsets from QS, each corresponding to approximately ⅛ of the QS daily total and comprising those bins with the highest incidence of delta and of sigma activities, respectively. Therefore, QSD and QSS are not a priori mutually exclusive and do not represent a staging of QS with fixed criteria. They simply denote those fractions of QS particularly rich in delta or sigma activities. In this manner, QSD can still be equated to those stages of human QS that are rich in delta activity, but QSS, unlike stage 2 in humans, stands positively for a higher incidence of spindles, reflecting more directly the activity of spindle generating mechanisms (26,27). The sizes of QSD and QSS are such that they represent a fraction of the day similar to that occupied by AS, a desirable situation for comparing distributions.

Long-term quantitative assessment of sleep variables presupposes an automated recording system (1,4,28–31). Our system is based on the detection of wave patterns and thus imitates the feature extraction process of visual scoring. Our results tend to converge with those of other long-term studies of sleep in the rat in terms of reported daily amounts of main states and in terms of their general temporal profiles (10,14,17,18,25,31–40). In a previous report (5) we

discussed the reliability of the system in terms both of detecting the relevant electrographic elements and of scoring bins as belonging to a given state. The percentage of disagreement between human and automated scoring is typically very low, and most of it can be attributed to misscoring some bins with a moderate amount of movements as wakefulness.

We aimed at determining the expected values of several variables that measured the location and dispersion of state distributions. We also wanted to assess their spontaneous intra- and interindividual variability, in order to obtain a background against which to interpret data from studies based on manipulations expected to change sleep distribution or migrate state location. We have presented the standard deviation of individual averages and the mean of individual standard deviations, because we were concerned with estimating expected variability rather than with analysis of variance, which would just confirm the biologically unsurprising fact that measurements within individuals are significantly more similar than between individuals.

Distributions of states followed two patterns. W and QS had a period of higher incidence that closely coincided with the dark and light phases, respectively, doubling that of the nonpreferred phase. The increase could anticipate in 1 hour the actual beginning of the phase. There was a moderate but consistent higher proportion of QS in the first half of the lights-on phase and of W in the second half of the dark phase, a fact that cannot be attributed to the third party AS. Accordingly, the mean and median angles of QS anticipated midday and those of W were delayed from midnight by approximately ½ hour, whereas both states had almost identical measures of concentration.

A different distribution was seen in the cases of AS and QSD. These states were much more clustered near their mean angle, as indicated by their mean vectors and quartile deviations. QSD was located at the beginning of the QS episode and its distribution was particularly leptokurtic. Its light : dark partition had a high interindividual variability because of its relation to the also inconstant degree in which QS anticipates the lights-on phase. On the other hand, AS reaches its highest incidence in the second half of the lights-on phase after a smoother increase. A similar course is followed by QSS, which reaches a maximum still later in the lights-on phase, but the amplitude of QSS modulation is less pronounced than that of AS.

The relative positions of the three measures of central tendency, mode, median and mean angles, can be taken as an indication of the skewness of the distributions. In QSD the mode angle is followed by the median angle and the mean angle, indicating that it tends to rise sharply and decline more slowly, whereas in AS and W the order is reversed, indicating a smoother shoulder at the rising slope. These features can be appraised better in the graphs of the hourly grand averages across rats shown in Fig. 2.

The graphs of the hourly grand averages are a result both of the shapes of individual distributions and of their variability. They are smoother than individual hourly averages and much more so than the single-day hourly distributions, such as the ones shown in Fig. 1. As a matter of fact, because of the ultradian modulation of many states and subsets, it is in the hourly average of several days where the assumptions of a von Mises distribution become particularly valid.

The fraction occupied by the two subsets within QS indicates a higher relative propensity to QSD at the end of the dark phase and beginning of the lights-on phase and to QSS in the first half of the dark phase. In this respect, it may be relevant to recall that human stage 2 has a lower arousal threshold. The differences in the configuration of sleep also concern AS very significantly, because it occupies a large fraction of the second half of the lights-on phase and of the first half of the dark phase. At least within the single light schedule considered for this report, the time courses of QSS and AS are similar between themselves and opposite to that of QSD.

The fact that spindle activity markedly increased towards the end of the sleep predominant phase suggests that mechanisms that enhance spindle generation by the reticular thalamic nucleus must operate beyond the mere release of its blockage by arousal (27).

In humans, sigma density increases throughout the night between consecutive QS/AS cycles (41). The increase of QSS throughout the sleep-predominant phase constitutes then a third significant similarity between human sleep and rat sleep, together with the gathering of deep delta-rich sleep at its beginning and the concentration of AS in its second half. Because humans and rats go through one phase of the light : dark cycle sleeping, spindle activity may contribute to maintain and prolong the sleep period once the restorative function associated with delta activity has been fulfilled.

Acknowledgements: Thanks are due to Guido del Pino for comments about the manuscript. We are grateful to Alexandra Silva for secretarial assistance. This work was supported by Grant FONDECYT 966-90.

REFERENCES

1. Vivaldi EA, Pastel RH, Bakalian MJ, Fernstrom JD. A microcomputer-based sleep system: data acquisition and system calibration programs. *Brain Res Bull* 1988;20:133–8.
2. Borbély AA. A two process model of sleep regulation. *Human Neurobiol* 1982;1:195–204.
3. Cowey A, Perry VH. The projection of temporal retina in rats,

studied by retrograde transport of horseradish peroxidase. *Exp Brain Res* 1979;35:457–64.
4. Vivaldi EA, Pastel RH, Fernstrom JD, Hobson JA. Long term stability of rat sleep quantified by microcomputer analysis. *Electroencephalogr Clin Neurophysiol* 1984;58:253–65.
5. Roncagliolo M, Vivaldi EA. Time course of rat sleep variables assessed by a microcomputer-generated data base. *Brain Res Bull* 1991;27:573–80.
6. Mardia KV. *Statistics of directional data.* London: Academic Press, 1972.
7. Batschelet E. *Circular statistics in biology.* London: Academic Press, 1981.
8. Zar JH. *Biostatistical analysis.* Englewood Cliffs: Prentice-Hall, 1984.
9. Nelson W, Liang Tong Y, Lee JK, Halberg F. Methods for cosinor-rhythmometry. *Chronobiologia* 1979;6:305–23.
10. Borbély AA, Neuhaus HU. Circadian rhythm of sleep and motor activity in the rat during skeleton photoperiod, continuous darkness and continuous light. *J Comp Physiol* 1978;128:37–46.
11. Rechtschaffen A, Kales A, eds. *A manual for standardized terminology, techniques and scoring system for sleep stages of human subjects.* Los Angles: UCLA Brain Information Service/ Brain Research Institute, 1968.
12. Carskadon MA, Rechtschaffen A. Monitoring and staging human sleep. In: Kryger MH, Roth T, Dement WC, eds. *Principles and practice of sleep medicine.* Philadelphia: Saunders, 1989: 665–83.
13. Michel F, Klein M, Jouvet D. Valatx JV. Etude polygraphique du sommeil chez le rat. *C R Séances Soc Biol* 1961;155:2389–92.
14. Van Twyver H. Sleep patterns of five rodent species. *Physiol Behav* 1969;4:901–5.
15. Timo-Iaria C, Negrao N, Schmidek WR, Hoshino K, Lobato de Menezes CE, da Rocha TL. Phases and states of sleep in the rat. *Physiol Behav* 1970;5:1057–62.
16. Rosenberg RS, Bergmann BM, Rechtschaffen A. Variations in slow wave activity during sleep in the rat. *Physiol Behav* 1976; 17:931–8.
17. Rosenberg RS, Bergmann BM, Jeong Son H, Arnason BG, Rechtschaffen A. Strain differences in the sleep of rats. *Sleep* 1987;10:537–41.
18. Trachsel L, Tobler I, Borbély AA. Electroencephalogram analysis of non-rapid eye movement sleep in rats. *Am J Physiol* 1988;R27–R37.
19. Richardson GS, Moore-Ede MC, Czeisler CA, Dement WC. Circadian rhythm of sleep and wakefulness in mice: analysis using long-term automated recording of sleep. *Am J Physiol* 1985;248:R320–R330.
20. Van Gelder RN, Edgar DM, Dement WC. Real-time automated sleep scoring: validation of a microcomputer-based system for mice. *Sleep* 1991;14:48–55.
21. Pellet J, Béraud G. Organisation nycthémérale de la veille et du sommeil chez le cobaye (Cavia porcellus). Comparaisons interespécifiques avec la rat et le chat. *Physiol Behav* 1967;2:131–7.
22. Sterman MB, Knauss, T, Lehmann D, Clemente CD. Circadian sleep and waking patterns in the laboratory cat. *Electroencephalogr Clin Neurophysiol* 1965;19:509–17.
23. Ursin R. The two stages of slow wave sleep in the cat and their relation to REM sleep. *Brain Res* 1968;11:347–56.
24. Ursin R. Sleep stage relations within the sleep cycles of the cat. *Brain Res* 1970;20:91–7.
25. Zepelin H. Mammalian sleep. In: Kryger MH, Roth T, Dement WC, eds. *Principles and practice of sleep medicine.* Philadelphia: Saunders, 1989:30–49.
26. Steriade M, Llinás R. The functional states of the thalamus and the associated neuronal interplay. *Physiol Rev* 1988;68:649–742.
27. Steriade M, Gloor P, Llinás RR, Lopes da Silva FH, Mesulam M-M. Basic mechanisms of cerebral rhythmic activities. *Electroencephalogr Clin Neurophysiol* 1990;76:481–508.
28. Gottesmann C, de Mendoza JJ, Lacoste G, Lallement B, Rodrigues L, Tasset M. Etude sur l'analyse et la quantification automatiques des différents états de veille et de sommeil chez le rat. *C R Hebd Acad Seances Paris* 1971;272:301–2.
29. Johns TG, Piper DC, James GW, Birtley RD, Fisher M. Automated analysis of sleep in the rat. *Electroencephalogr Clin Neurophysiol* 1977;43:103–5.
30. Smith JR. Automated analysis of sleep EEG data. In: Lopes da Silva FH, Storm van Leeuwen W, Remond A. eds. *Handbook of electroencephalography and clinical neurophysiology* (revised series), vol. 2. Amsterdam: Elsevier, 1986:131–47.
31. Ruigt GS, van Proosdij JN, van Delft AM. A large scale, high resolution, automated system for rat sleep staging. I. Methodology and technical aspects. *Electroencephalogr Clin Neurophysiol* 1989;73:52–63.
32. Mouret J, Coindet J, Chouvet G. Effet de la pinéalectomie sur les états et rythmes de sommeil du rat mâle. *Brain Res* 1974; 81:97–105.
33. Mouret J, Coindet J, Debilly G, Chouvet G. Suprachiasmatic nuclei lesions in the rat: alterations in sleep circadian rhythms. *Electroencephalogr Clin Neurophysiol* 1978;45:402–8.
34. Borbély AA, Neuhaus HU. Daily pattern of sleep, motor activity and feeding in the rat: effects of regular and gradually extended photoperiods. *J Comp Physiol* 1978;124:1–14.
35. Borbély AA, Neuhaus HU. Sleep-deprivation: effects on sleep and EEG in the rat. *J Comp Physiol* 1979;133:71–87.
36. Mistlberger R, Bergmann BM, Waldenar W, Rechtschaffen A. Recovery sleep following sleep deprivation in intact and suprachiasmatic nuclei-lesioned rats. *Sleep* 1983;6:217–33.
37. Vivaldi EA, Roncagliolo M, Aylwin M. Temporal structure of the sleep–wakefulness cycle in the rat. *Arch Biol Med Exp* 1984; 17:R192.
38. Trachsel L, Tobler I, Borbély AA. Sleep regulation in rats: effects of sleep deprivation, light, and circadian phase. *Am J Physiol* 1986;251:R1037–R1044.
39. Bergmann BM, Mistlberger RE, Rechtschaffen A. Period–amplitude analysis of rat electroencephalogram: stage and diurnal variations and effects of suprachiasmatic nuclei lesions. *Sleep* 1987;10:523–36.
40. Franken P, Derk-Jan D, Tobler I, Borbély AA. Sleep deprivation in rats: effects on EEG power spectra, vigilance states, and cortical temperature. *Am J Physiol* 1991;261:R198–R208.
41. Azumi K, Shirakawa S. Characteristics of spindle activity and their use in evaluation of hypnotics. *Sleep* 1982;5:95–105.